ELSEVIER
Thermochimica Acta 285 (1996) 167–179
thermochimica acta

Temperature-programmed reduction of calcined chromia-coated alumina and silica catalysts: probing chromium (VI)–oxygen species

Mohamed I. Zaki[a,]*, Nasr E. Fouad[b], Geoffrey C. Bond[c], Saad F. Tahir[c]

[a] *Department of Chemistry, Faculty of Science, Kuwait University, P.O. Box 5969-Safat, Kuwait*
[b] *Department of Chemistry, Faculty of Science, Minia University, El-Minia 61519, Egypt*
[c] *Department of Chemistry, Faculty of Science, Brunel University, Uxbridge UB8 3PH, UK*

Received 6 November 1995; accepted 28 January 1996

Abstract

Chromia-coated alumina and silica, containing 0.5, 5 and 10 wt% Cr_2O_3, have been prepared by adding $Cr(NO_3)_3$ solution to a suspension of the support in NH_4OH followed by calcination at 600°C. Temperature-programmed reduction (TPR) of a corresponding unsupported chromia showed peaks at 370 and 490°C, due to reduction of surface chromate groups; commercial α-Cr_2O_3 showed no hydrogen uptake. TPR measurements on the chromia-coated supports, together with information from the literature, lead to the conclusion that reducible chromate groups are present on the surface in a variety of forms having different degrees of ease of reduction and hydrolysis, their numbers and structures depending on Cr content and the nature of the support. H_2 uptakes are markedly less than expected on the basis of hydrazine titration of surface excess oxygen. The reactivities of surface chromate groups may be understood on the basis of difference in the polarizability of metal-oxygen bonds in the support.

Keywords: Calcined chromia; Chromia; Chromia/alumina; Chromia/silica; Temperature programmed reduction

1. Introduction

Calcined chromia catalysts, i.e. pretreated under oxidizing conditions whether supported ot unsupported, perform far more actively in redox processes than chromia

---

* Corresponding author.

PII S0040-6031(96)02874-2

catalysts prepared under non-oxidizing conditions [1–3]. However, their industrial application is hampered by justifiable environmental reservations. Surface chromates [$Cr^{VI}O$] thus generated on the calcined catalyst are highly toxic, and are therefore classified as being detrimental to the atmosphere [4]. However, the presence of intimately coupled Cr^{VI}–Cr^{III} site-pairs has been considered [5, 6] to facilitate electron migration across the surface and, hence, to optimize the redox activity of chromia catalysts.

Careful studies have been carried out [7–11] focusing on the course of solid-state reactions leading to formation of chromates from various Cr^{III}-containing precursors, and the topochemical events involved therein. The structure and stoichiometry of surface chromates have been elucidated, applying a wide range of spectroscopic [11–17] and magnetic [5,18] analytical techniques and methods. Quantification of surface chromates has been carried out, implementing both chemical [19] and physicochemical [20, 21] methods. However, the powerful aid of temperature-programmed reduction (TPR) measurements, particularly in probing such high valent metallates [22], has not been sufficiently exploited in examining calcined chromates [23,24].

In summary, monomeric (CrO_4^{2-}) and polymeric chromates ($Cr_{1+x} + O_4 + 3x^{2-}$) have been observed on surfaces of calcined chromia catalysts [13, and references cited therein]. The chromates established on crystalline chromia (α-Cr_2O_3) particles have been claimed [11, 15, 16, 25] to be more stable, chemically and thermally, than those anchored directly onto silica and alumina supports.

In a previous study [23], TPR was performed on calcined chromia supported on silica and alumina via impregnation from Cr^{III} solutions. The results were in line with other characterization results [11], in probing chromates of varied structures and thermochemical stabilities [23]. In the present study, TPR is used to probe chromates generated by calcination of similarly supported chromia, but loaded by coating the support particles with chromia gel. The motive of this move was primarily the different structures and stabilities observed for chromates in the coated materials [11] as compared to the impregnated ones [13]. The present TPR study involved a set of precharacterized [13] chromia-coated silica and alumina materials, which were obtained by calcination at 600°C of variously loaded (0.5–10 wt% Cr_2O_3) parents. The TPR results are assessed on the basis of other characterization results which have been reported earlier [13], and compared with reported TPR results for supported chromia by impregnation [23]. The study aims at a better understanding of the surface attributes and stability of chromates in calcined chromia catalysts.

2. Experimental

2.1. Materials

Degussa Aluminiumoxid C ($S_{BET} = 135$ m^2 g^{-1}, $V_p = 0.34$ ml g^{-1}) and Davison Silica Gel (calcined for 3 h at 400°C before use, $S_{BET} = 265$ m^2 g^{-1}, $V_p = 1.3$ ml g^{-1})

were used as supports. Analogously to McDaniel and Burwell [26], the supports were coated with chromia gel to various loading levels (0.5–10 wt% Cr_2O_3) by adding dropwise a calculated amount of 0.1 M $Cr(NO_3)_3 \cdot 9H_2O$ (99.8% pure BDH) solution of the appropriate amount of the support, being continuously stirred and simmered at 85°C in 200 ml of NH_4OH solution (pH 9.2). The slurries obtained were left overnight in contact with the mother liquor at room temperature (RT), and then filtered and dried at 80°C to constant weight (36 h). The dried materials were calcined at 600°C (encompassing commercial conditions) in a still atmosphere of air, and the products were kept dry over P_2O_5 till further use. For clarity, the calcination products are indicated below by designation referring to the loading level and support. Thus, CrCAl10 indicates calcined chromia-coated alumina containing 10 wt% Cr_2O_3, whereas $CrCSi_5$ denotes calcined chromia-coated silica of 5 wt% Cr_2O_3.

For control purposes, a chromia sample (designated CrC) was synthesized, in the absence of the support, under the same preparative conditions. They were similarly filtered, dried and calcined at 600°C for 5 h.

2.2. *TPR measurements*

The TPR equipment has been described in detail elsewhere [27]. Small amounts of test samples (29–240 mg) and a 5% H_2/Ar gas mixture were used (flow rate, 40 ml min^{-1}; pressure, 760 Torr, 1 Torr = 133.3 Pa). Heating up to 1000°C was effected at a rate of 5°C min^{-1}.

3. Results

3.1. *TPR profiles of the unsupported chromia*

CrC gives rise to a TPR profile (Fig. 1) consisting of maxima at 370 and 490°C, and a minimum at 800°C. The TPR of a commerical α-Cr_2O_3 (BDH, UK) showed only a very small minimum at ≤ 750°C (see also Fig. 1). Other research [28] has concluded that exposed Cr^{III} in crystalline α-chromia may be reduced at temperatures well below 750°C, provided CO (rather than H_2) is used as the reductant. The CO_2 thus produced is much more stable than H_2O to subsequent reduction by Cr^{II}. Accordingly, the maxima observed at 370 and 490°C for CrC are reduction peaks reflecting either two overlapping single-step processes involving two different high-valent CrO_x species, or a two-step process involving one-and-the-same CrO_x species. However, the minimum at 800°C is a hydrogen desorption peak.

Previous characterization studies [15, 17, 29] of calcined chromia-derived catalyst at temperatures ≥ 600°C are unanimous in assigning reducible CrO_x species to chromates (mainly as surface species). Accordingly, the total hydrogen consumption (10^{-5} mol H_2 g^{-1}) determined from the two reduction peaks was used to calculate redox-related information for chromates in CrC, and the results are set out in Table 1.

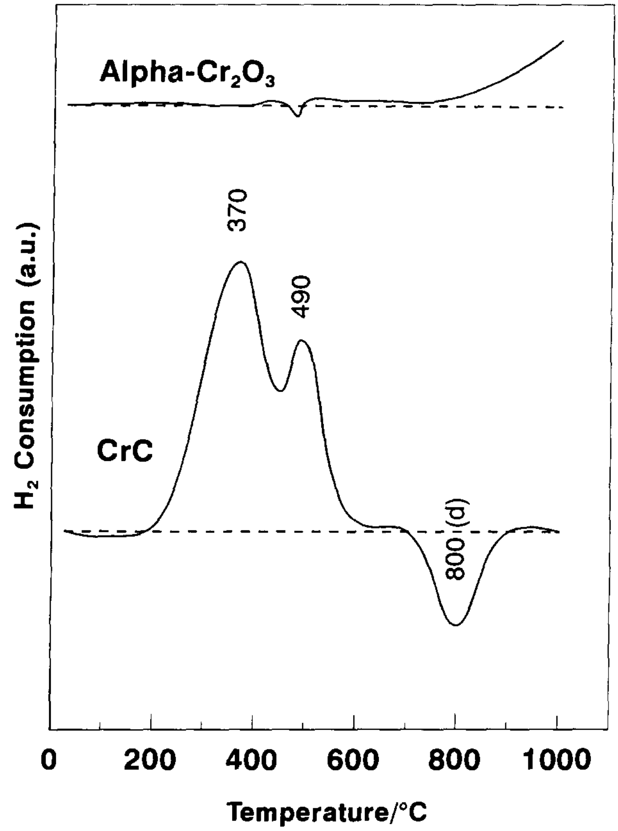

Fig. 1. TPR profiles for unsupported chromia (CrC) obtained by calcination of chromia gel at 600°C for 5 h, and a commercial chromia (α-Cr_2O_3). Hydrogen consumption is in arbitrary units (a.u.).

3.2. *TRP profiles of chromia-coated silicas*

TPR profiles for the CrCSi materials are presented in Fig. 2, and results derived therefrom are compared in Table 1. The profiles are broadly similar in showing reduction peaks at 390–410°C and 450–470°C and a desorption peak at 930–980°C. Only the CrCSi5 sample gives rise to a peak at the low temperature of 330°C. Since pure silica does not show detectable reduction under similar conditions [23], the peaks are due solely to species in the chromia coating.

It is clear from Table 1 that the total hydrogen consumption increases with the loading of chromia. However, the chromia-specific results calculated therefrom (Table 1) show the oxidation (%) of chromia during the calcination to decrease as the loading increases. This may be explained by the inverse proportionality between the chromia dispersion and the loading.

Table 1
Results derived from TPR profiles for various materials

Materials	T_{max}[a] °C	Total H_2 consumption/ (10^{-5} mol H_2 g^{-1})	Oxygen consumption[b] (10^{-5} mol O_2 g^{-1})	Active oxygen[c]/ (mole O/mole $CrO_{1.5}$)	Oxidation[d]/%
CrC	370 490	44	22	0.03	3
CrCSi0.5	410 470	4	2	0.60	53
CrCSi5	330 390 470	8	4	0.12	11
CrCSi10	410 450	21	11	0.16	14
CrCAl0.5	570	18	9	2.71	100[e]
CrCAl5	320 565	16	8	0.24	21
CrCAl10	550	8	4	0.06	4

[a] Temperatures at which reduction rate peaks; thus, desorption peaks monitored in Figs. 1–3 are not included.

[b] Calculated consumption of oxygen on the basis of the corresponding total hydrogen consumption.

[c] Molar proportion of excess (active) oxygen per mole of the irreducible moiety of chromia ($= CrO_{1.5}$), calculated on the basis of the fact that the eventual reduction product at ≤ 750°C is Cr_2O_3 and that chromates are the only reducible species present.

[d] Approximated by relating the amount of oxidized chromia, as derived from the amount of oxygen consumed, to the total amount of chromia per g of material.

[e] Symbolises an almost complete oxidation of chromia coating; the actual amount calculated is meaningless (> 100%).

3.3 TPR profiles of chromia-coated aluminas

Figure 3 compares the TPR profiles shown by CrCAl materials; results derived therefrom are given in Table 1. The three profiles exhibit a similar high-temperature peak at 550–570°C and a desorption peak at 920–930°C. The notable broadness and shape asymmetry of the high-temperature reduction peak may account for a reduction behaviour at 450–500°C. They differ however in that CrCAl.5 and CrCAl10 both display low-temperature desorption peaks (320–430°C), while CrCAl5 shows only a single strong reduction peak at 320°C. Also in these test materials, the alumina does not show a reduction of any substance under similar conditions [23]. Hence, the peaks are ascribed exclusively to the chromia coating.

The derived results (Table 1) agree with those for the CrCSi materials in allocating the highest extent of oxidation to the material of lowest loading, i.e. CrCAl.5. Except for the case of CrCAl10, the oxidation of the coating is easier on alumina than silica. The results for the two series (CrCAl and CrCSi) disagree in showing the total hydrogen consumption by the CrCAl materials to decrease as the loading level increase. This may

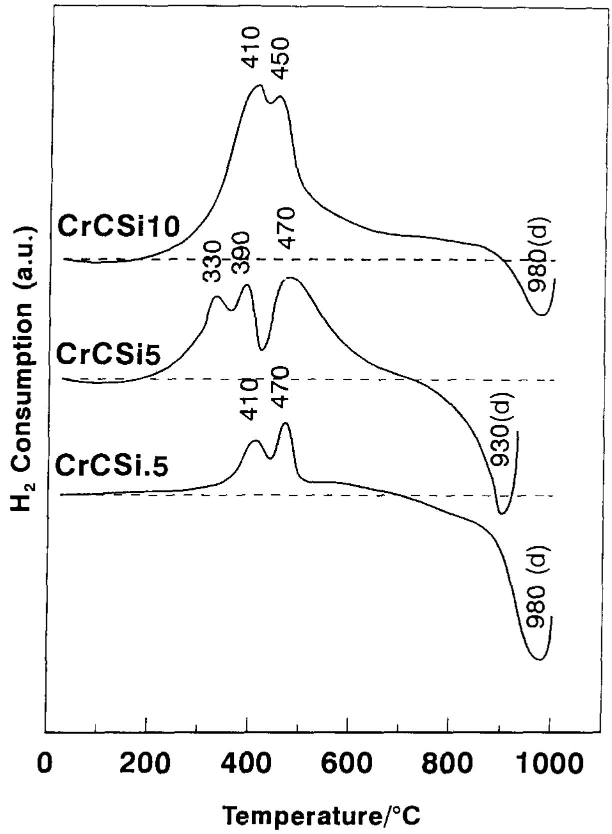

Fig. 2. TPR profiles for the chromia-coated silicas indicated.

imply a lower reducibility of the CrO_x species in the CrCAl materials than those in the CrCSi ones.

4. Discussion

4.1. Surface and bulk characteristics of the materials

The present materials were the subject of a previous characterization study [13], and relevant results are reviewed in Table 2. It is obvious that the 600°C calcination of the unsupported chromia (CrC) results predominantly in α-Cr_2O_3 particles exposing a partially oxidized surface of 52 $m^2\ g^{-1}$ and a trace amount of γ-Cr_2O_{3+x}. The oxidized species are mainly surface chromates anchored onto the α-chromia crystalline lattice, whereas γ-Cr_2O_{3+x} exists as a low concentration of bulk chromates bound to noncrystalline chromia (chromium chromate) [5].

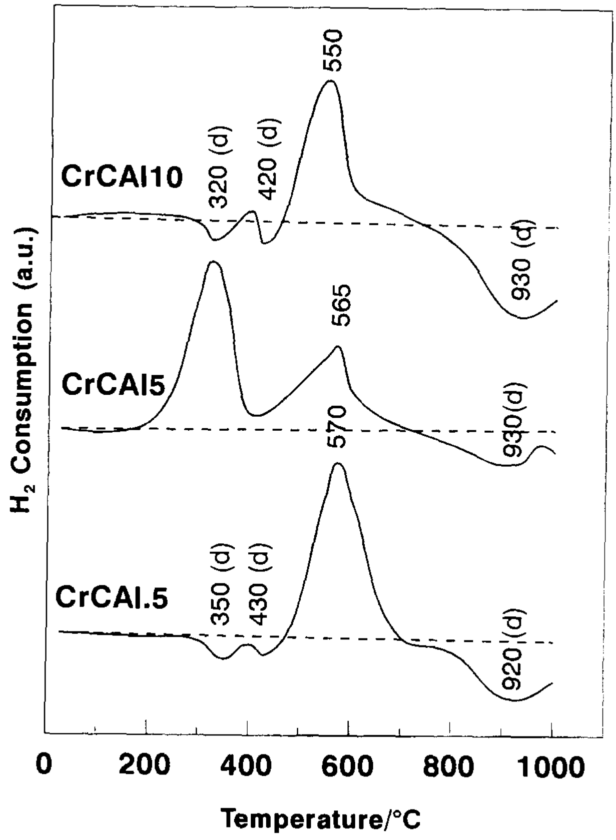

Fig. 3. TPR profiles for the chromia-coated aluminas indicated.

Upon coating silica with increasing amounts of chromia (0.5–10 wt%) and subsequent calcination at 600°C, the products at up to 5 wt% Cr_2O_3 showed a decrease in surface area (from 265 down to 220 $m^2\ g^{-1}$); however at 10 wt% Cr_2O_3, the surface area had increased (to 368 $m^2\ g^{-1}$) to surpass that of the support (256 $m^2\ g^{-1}$). The latter behaviour must imply that the increase in loading leads to the formation of clumps, islands and/or build-up of 3-dimensional chromia phase [13]. According to Dollimore and Pearce [30], the higher average value (295 $m^2\ g^{-1}$) of the surface area calculated (S^c_{BET}, Table 2) for the coated support than that measured for the support itself ($S^m_{BET} = 265\ m^2\ g^{-1}$) confirms this view. Large α-Cr_2O_3 particles (average size, 0.5 μm) were evident in transmission electron micrographs taken previously for the CrCSi10 [31]. X-ray diffractometry [13] also identified crystalline α-Cr_2O_3 particles in both CrCSi5 and CrCSi10 as being the major detectable bulk chromia phase (Table 2). Accordingly, chromates established in CrCSi materials were characterized as being polymeric and anchored onto crystalline chromia and, to a much lesser extent, onto

Table 2
Surface and bulk characteristics of various materials, as determined and reported earlier [13]

Materials	Specific surface area/ $m^2\ g^{-1}$		Cr^{III}–oxygen species		Cr^{VI}–oxygen species	
	S^m_{BET}[a]	S^c_{BET}[b]	Type[c]	Proportion[d]	Type[c]	Proportion[d]
CrC	52	–	γ	*t*	cc	*s*
			α''	*d*		
CrCSi0.5	244	245	γ	*m*	pc	*j*
			α'	*j*		
CrCSi5	220	231	γ	*m*	pc	*m*
			α'	*m*	cc	*j*
			α''	*j*		
CrCSi10	368	408	γ	*t*	pc	*m*
			α'	*m*	cc	*d*
			α''	*d*		
CrCAl0.5	129	130	δ	*m*	mc	*j*
			β	*j*	cc	*t*
			γ	*t*		
			α'	*t*		
CrCAl5	117	123	γ	*m*	mc	*m*
			α'	*j*	cc	*j*
			α''	*t*		
CrCAl10	110	122	γ	*j*	mc	*m*
			α'	*m*	cc	*d*
			α''	*m*		

[a] Determined ($\pm 2\ m^2\ g^{-1}$) by BET analysis of N_2 adsorption isotherms measured at liquid nitrogen temperature [13].

[b] Calculated [13] using the relationship [30]: $S^c_{BET} = S^m_{BET}$ of material/1 – chromia content per g material).

[c] δ, isolated Cr^{III} species; β, Cr^{III} clusters; γ, γ-Cr_2O_{3+x}, α' noncrystalline chromia; α'', crystalline α-Cr_2O_3.

[d] *t*, trace; *m*, minor; *j*, major; *d*, dominate; *s*, sole.

[e] mc, monochromate/support; pc, polychromate/support; cc, chromium chromates, (i.e. mc/α'-chromia; pc/α''-chromia.

noncrystalline chromia and the silica support. Only in the lowest loaded CrSi0.5 were the polychromates seen to be bound essentially to the silica surface (Table 2)

Similarly, the close agreement between the average S^c_{BET} for the CrCAl materials (125 $m^2\ g^{-1}$, Table 2) and S^m_{BET} for the alumina support (130 $m^2\ g^{-1}$) can be accounted for by monolayer spreading of CrO_x species. Indeed, X-ray diffractometry detected [13] only a minor proportion of α-Cr_2O_3 particles in CrCAl10, and transmission electron microscopy measured [31] much smaller chromia crystallites (average size, 0.2 μm) than observed in CrCSi10 (0.5 μm).

The chromates were found [13] to be largely monomeric and anchored either onto alumina or amorphous chromia. The species found on chromia, i.e. chromium chromate, increased in proportion to the loading.

It is worth noting that neither X-ray diffractometry [13] nor electron microscopy [31] could detect crystalline interaction products of chromia with the respective supports in CrCSi and CrCAl materials.

4.2. TPR-characterized chromates

The TPR results are assessed in terms of the following experimental facts.

(i) The reducible species are exclusively chromates (Cr^{VI}–O). Chemical [13, 20] and physicochemical [13, 15, 18, 29] analyses of these and similar materials excluded the thermal stability of oxygen species of Cr^{IV} and Cr^{V} at $\geq 600^{\circ}C$.

(ii) The chromates are essentially surface species. Amounts of oxygen consumed corresponding to the total hydrogen uptakes (Table 1) are much less than those determined previously [13] by hydrazine titration of the total surface excess oxygen on the same set of materials. In fact, actual amounts of oxygen consumed are mostly less than those given in Table 1, since H_2 consumption is not necessarily equivalent to oxygen removal, i.e. H_2O formation.

(iii) Complex TPR profiles (Figs. 1–3; Table 1) can be accounted for by surface chromates bound to different substrates: noncrystalline chromia, α-chromia, silica and γ-alumina (Table 2). Thus, TPR probes only a part of the total amount of hydrazine-determined surface chromates [13]; and the amount of reducible chromates is mostly even less than the amount of hydrolysable, i.e. water-leachable, chromates [13]. Only in the case of CrCAl0.5 and CrCSi10 are the amounts of reducible and hydrolysable chromates comparable.

(iv) Surface chromates stabilized at 600°C comprise species that vary in their ease of reduction and of hydrolysis; the number and nature of such species being determined by the Cr content and the support. Mihajlova and Andreev [32] have also deduced the presence of chemically stable and unstable surface chromates in high-temperature calcination products of chromia gel.

Accordingly, the TPR peaks observed for all the materials can be grouped into three classes, each distinguished by a different temperature regime. These are given in Table 3, together with relevant characteristics of the reducible chromates involved. Thus, the TPR probes three different types of surface chromates, and Table 3 shows that the structure and chemistry of the substrate plays a decisive role in determining the

Table 3
Reducible chromate species as characterized by TPR results (present work) and other analytical results (previous work[13])

Reduction temp.:	320–410°C	450–490°C	550–570°C
Type	I	II	III
Substrate	SiO_2 and/or *Cry*. α-Cr_2O_3[a]	SiO_2 and/or *NCry*. chromia[a]	Al_2O_3 *NCry*. chromia[a]
Surface structure	Polychromates (*j*)[b] Monochromates (*m*)	Polychromates (*m*) Monochromates (*j*)	Monochromates (*d*)
Covalency	High	Medium	Low
Hydrolisability	Low	Medium	High
Reducibility	High	Medium	Low

[a] *Cry*, crystalline; *NCry*, non-crystalline.
[b] *j*; major; *m*, minor; *d*, dominat.

reducibility of the chromates supported thereon. Chromates anchored directly onto silica surfaces are more reducible (at < 500°C) than those bound to alumina surfaces (at > 500°C). However, chromates exposed on crystalline chromia are more reducible (at < 410°C) than those established on noncrystalline chromia (at > 410°C). Together with other characteristics observed previously [13], Table 3 can indicate that the higher the stability of the chromate of H_2 reduction, the lower it is to hydrolysis. These two opposing behaviours may be explained by correlating high reducibility-low hydrolysability with the high degree of convalency, i.e. high polarizability, assigned previously to the metal–oxygen bonds within the chromate structure. When traced back to the nature of the substrate, this correlation fits well with the electronically "*hard*" nature of alumina, in contrast to the electronically "*soft*" nature of silica [33]. This is because electronically soft supports have highly polarizable metal–oxygen bonds, which may create an electron-mobile environment for the reduction of metallates supported on them [34]. A quantum chemical study of supported chromates [35] has stressed the necessity for an explicit criterion for the interaction of the chromates with the support metal–oxygen bonds in order to simulate the catalytically active sites.

4.3. Tolerance of chromates to redox cycles

The above section indicates that surface chromates formed at 600°C on calcined chromia-containing materials might well have various chemical stabilities; it was then of interest to investigate their tolerance to redox cycles. A reduced CrCAl5 sample was therefore re-calcined by heating in air for 5 h and then re-reduced; TPR profiles for the fresh and re-calcined samples are compared in Fig. 4.

The TPR of the fresh sample detects (Fig. 3 and Table 3) chromates that are reducible at low temperature ($T_{max} = 322°C$) and high temperature ($T_{max} = 564°C$). Moreover, the presence of chromates reducible at intermediate temperature ($T_{max} \simeq 480°C$) cannot be ruled out. According to Table 3, the low-temperature species is most likely a polychromate exposed on crystalline chromia, whereas the high-temperature species is a monochromate anchored directly onto the alumina support. The suspected intermediate-temperature species is also, accordingly, a mono-/polychromate found on noncrystalline chromia.

The TPR of the re-calcined CrCAl5 indicates that the oxidation could restore reducible chromates on crystalline chromia (reversible species), shifting the maximum temperature of the reduction peak to a slightly higher value (360°C). In contrast, reducible chromates bound directly to the alumina surface, and those formed on noncrystalline chromia, were not restorable (irreversible species). These results confine the redox tolerance to surfaces of crystalline α-chromia, thus making them a promising catalyst for deep oxidation (combustion) processes which necessitate catalytic surfaces of a high tolerance to cyclic oxygenation–deoxygenation events [36]. Accordingly, the chemical and thermal stabilities of the active chromates (irreversible species) demand the maintenance of an oxygen-rich environment throughout the reaction. This condition may be fulfilled for some oxidation processes, but cannot apply to some others, e.g. oxidation of automobile emissions [37].

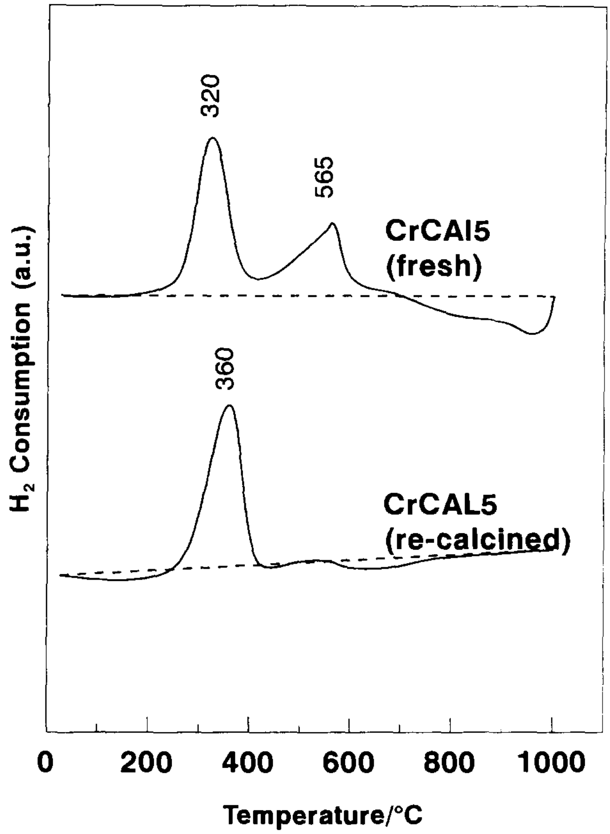

Fig. 4. TPR profiles for freshly calcined and re-calcined samples of CrCAl5. The re-calcination was also effected at 600°C for 5 h, following the reduction experiment.

4.4. Dependency of chromate stability on the loading technique of chromia

In an earlier TPR study of supported chromias [23], samples were prepared by impregnation of alumina and silica with $Cr(NO_3)_3 \cdot 9H_2O$ to 10 wt% Cr_2O_3 and subsequent calcination at 600°C for 5 h. Unlike the case with the present CrCSi10, the silica-supported material thus obtained was H_2-irreducible at temperatures below 773°C. However, the alumina- supported material showed a broad TPR band centred around 300°C, i.e. at a much lower temperature than that (550°C) observed for the reduction peak of the present CrCAl10. It is worth mentioning that the materials derived from the impregnated parents also exposed detectable chromates [11]. Accordingly, the earlier study [23] concluded, in apparent contrast to the present study, that chromates are most stabilized to hydrogen reduction (and to hydrolysis) when established on crystalline chromia.

It is obvious that the differences between the TPR behaviours of the present and previous samples are due to: (i) the different loading techniques of the parent Cr^{III}

species (coating vs. impregnation); and (ii) the different chemical compounds of the parents (chromia gel vs. chromium nitrate). The latter difference has manifested itself strongly in the fact that unsupported calcined product of the nitrate showed no TPR profiles at $< 773°C$, whereas the present CrC did (Fig. 1). The crystalline structure of the two unsupported materials consisted essentially of α-Cr_2O_3, but of evidently different crystallinities (CrC was less crystalline). Moreover, markedly different redox and solid-state chemical events were shown by the parent compounds during the thermal genesis of the two unsupported chromias (Ref. [13] for chromia gel and Ref. [11] for chromium nitrate).

Impregnation of Cr^{III} aquated species $[Cr(H_2O)_5(OH)^{2+}]$ involves strong adsorptive interactions with silica, but much weaker such interactions occur with alumina [32] due to the disparate interfacial chemistries at the different oxide/solution interfaces [38]. In contrast, coating of the support particles with chromia gel (the present case) involves essentially mechanical deposition, thus making interfacial adsorptive interactions less important. Solid/solid interactions triggered during the subsequent calcination become the most important parameter in determining the surface structure of the coated samples. The balance between the importance of primary adsorptive interactions and that of the subsequent solid/solid interactions to the surface structure is tilted towards the latter on switching from "*impregnation*" to "*coating*" as the loading technique. Consequently, the thermal and chemical stabilities of surface chromates generated in the two sets of materials will vary, as is demonstrated in the present work.

References

[1] C.P. Poole, Jr. and D.S. Maclver, Adv. Catal., 17 (1967) 223.

[2] R.L. Burwell, Jr., G.L. Haller, K.C. Taylor and J.F. Read, Adv. Catal., 20 (1969) 1.

[3] M.P. McDaniel, Adv. Catal., 33 (1985) 47.

[4] Fact Sheet No. 210, a publication of California Department of Toxic Substance Control, Office of Pollution Prevention and Technology, Sacramento/CA, USA, May 1993.

[5] A. Ellison, J.O.V. Oubridge and K.S.W. Sing, Trans. Faraday Soc., 66 (1970) 1004.
A. Ellison and K.S.W. Sing, J. Chem. Soc., Faraday Trans. 1, 74 (1987) 2807.

[6] R.B. Fahim, M.I. Zaki and R.M. Gaber, Appl. Catal., 4 (1982) 189; Surf. Technol., 12 (1981) 317.

[7] H. Park, Bull. Chem. Soc. Jpn., 45 (1972) 2749; 45 (1972) 2735.

[8] M.I. Zaki and R.B. Fahim, J. Therm. Anal., 31 (1986) 825.

[9] M.I. Zaki and N.E. Fouad, Thermochim. Acta, 95 (1985) 73.

[10] N.E. Fouad, Bull. Fac. Sci. Assiut Univ., 22 (1993) 55.

[11] N.E. Fouad, H. Knözinger, M.I. Zaki and S.A.A. Mansour, Z. Phys. Chem. (München), 171 (1991) 75.

[12] A. Zecchina, E. Garrona, G. Ghiotti, C. Morterra and E. Borello, J. Phys. Chem., 79 (1975) 966.
A. Iannibello, S. Marengo, P. Tirtarelli, G. Morelli and A. Zecchina, J. Chem. Soc., Faraday Trans. 1, 80 (1984) 2209.

[13] M.I. Zaki, N.E. Fouad, J. Leyrer and H. Knözinger, Appl. Catal., 21 (1986) 359.

[14] P.J.M. Carrott and N. Sheppard, J. Chem. Soc., Faraday Trans. 1, 79 (1986) 2425.

[15] V.V. Mikolaichuk, E. Stoch, I.V. Babich, A.V. Isarov, Yu.V. Plyuto and A.A. Chuiko, Dokl. Nauk (Engl. Trans.), 320 (1991) 1408.

[16] B.M. Weckhuysen, L.M. de Ridder and R.A. Schoonheydt, J. Phys. Chem., 97 (1993) 4756.

[17] R. Rahman, M.H. Mohamed, M. Ahmed and A.M. Aitani, Appl. Catal., 121 (1995) 203.

[18] L.L. van Reijen and P. Cossee, Faraday Discuss., (1966) 277.

[19] R.B. Fahim, R.M. Gabr, M.I. Zaki and S.A.A. Mansour, J. Colloid Interface Sci., 81 (1981) 468. R.B. Fahim, M.I. Zaki and N.H. Yacoub, J. Colloid Interface Sci., 88 (1982) 502.
[20] J. Deren, J. Haber, H. Podgorecka and J. Burzyk, J. Catal., 2 (1963) 161.
[21] H.L. Lugo and J.H. Lunsford, J. Catal., 91 (1985) 155; D.L. Myers and J.H. Lunsford, J. Catal., 92 (1985) 260.
[22] H.M. Ismail, M.I. Zaki, G.C. Bond and R. Shukri, Appl. Catal., 72 (1991) L1.
[23] N.E. Fouad, H. Knözinger and M.I. Zaki, Z. Phys. Chem. (München), 186 (1994) 231.
[24] E. Ehrhardt, M. Richter, U. Roost and Öhlmann, Appl. Catal., 17 (1985) 23.
[25] V.V. Mikolaichuk, A.V. Isarov, Yu. V. Plyuto and A.A. Chuiko, Teoreticheskaya i Eksperimental'naya Khim. (Engl. Transl.), 27 (1991) 726.
[26] M.P. McDaniel and R.L. Burwell, Jr., J. Catal., 36 (1974) 404.
[27] G.C. Bond, J.P. Zurita, S. Flamerz, P.J. Gellings, H. Bosch, J.G. van Ommen and B.J. Kip, Appl. Catal., 7 (1986) 361.
[28] A. Zecchina, S. Coluccia, E. Guglieminotti and G. Ghiotti, J. Phys. Chem., 75 (1971) 2774.
[29] K. Jagannathan, A. Srinivasan and C.N.R. Rao, J. Catal., 69 (1981) 418.
[30] D. Dollimore and J. Pearce, Powder Technol., 25 (1980) 71.
[31] T. Baird and M.I. Zaki, Inst. Phys. Conf. Ser. No. 90, (1987), Chapter 2, pp. 43–46.
[32] D. Mihajlova and A. Andreev, Bull. Bulg. Acad. Sci., 2 (1976) 265.
[33] R.G. Pearson, J. Am. Chem. Soc., 85 (1963) 3533; Chem. Br., 3 (1976) 103.
[34] A. Corma, G. Sastre, R. Viruela and C. Zicovich-Wilson, J. Catal., 136 (1992) 521.
[35] I.V. Plyuto, A.P. Shpak, Yu. V. Plyuto and A. Chuiko, Teoretocheskaya i Eksperimental'naya Khim. (Engl. Transl.), 24 (1988) 602.
[36] R. Prasad, L.A. Kennedy and E. Ruckenstien, Catal. Rev. Sci. Eng., 26 (1984) 1.
[37] F. Nakajima, Catal. Today, 10 (1991) 1.
[38] M.I. Zaki, S.A.A. Mansour, F. Taha and G.A.H. Mekhemer, Langmuir, 8 (1992) 727.